

Supporting Information

Synthesis of functionalized 3D hierarchical porous carbon for high-performance supercapacitor

Long Qie,^a Weimin Chen,^a Henghui Xu,^a Xiaoqin Xiong,^a Yan Jiang,^a Feng Zou,^a Xianluo Hu,^a Ying Xin,^b Zhaoliang Zhang^b and Yunhui Huang*^a

^aKey Laboratory for Advanced Battery Materials and System, Ministry of Education; School of Materials Science and Engineering, Huazhong University of Science and Technology, Wuhan, Hubei 430074, China

^bShandong Provincial Key Laboratory of Fluorine Chemistry and Chemical Materials, School of Chemistry and Chemical Engineering, University of Jinan, Jinan 250022, China

Content:

Figure S1. SEM images of THPC.

Figure S2. SEM images of AC (obtained through annealing the mixture of PPy and KOH at 700 °C).

Figure S3. Raman spectrum of PPy microsheets.

Figure S4. Nitrogen adsorption-desorption isotherms and pores size distribution (PSD, the inset) of PPy microsheets.

Figure S5. Survey XPS spectra of THPC.

Figure S6 Electrochemical performances of THPC as anode material for lithium-ion batteries: (a) discharge/charge curves at 0.2 C; (b) capacity over cycling at different rates; (c) cyclability and coulombic efficiency at 5 C; (d) impedance spectra of THPC after the 1st, 10th, 50th, 100th and 500th cycle at 5 C.

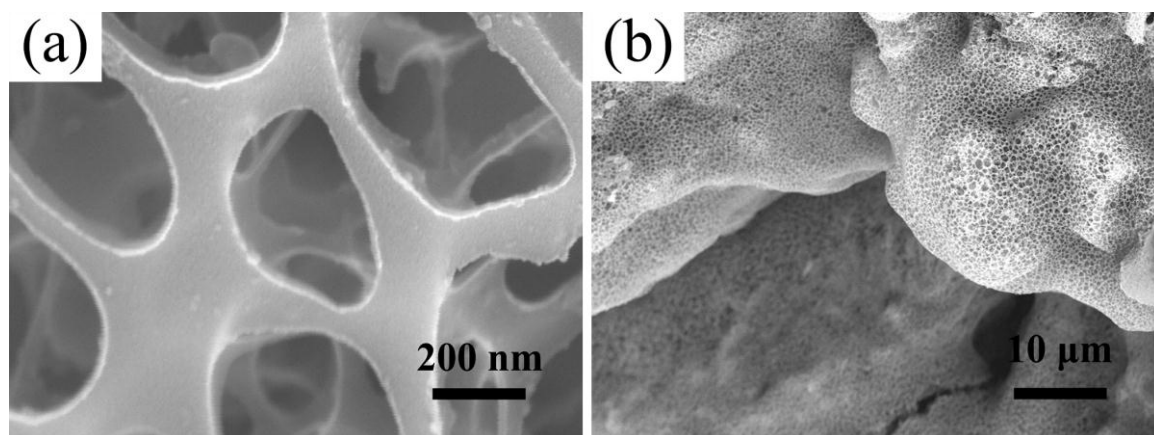


Figure S1. SEM images of THPC.

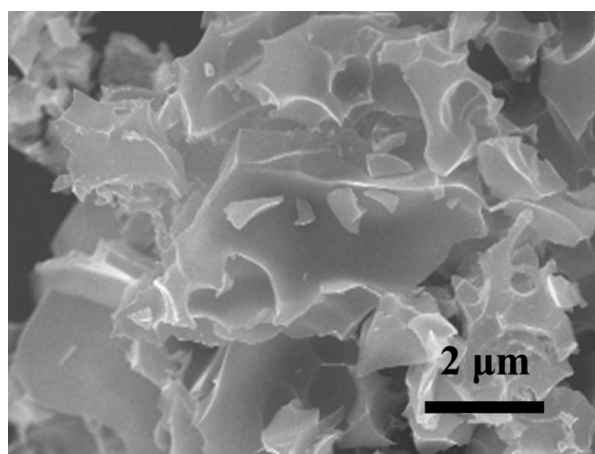


Figure S2. SEM images of AC (obtained through annealing the mixture of PPy and KOH at 700 °C).

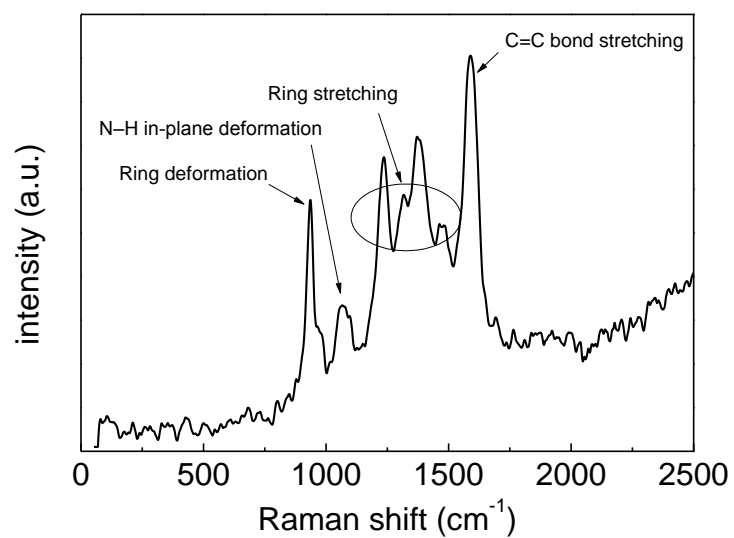


Figure S3. Raman spectrum of PPy microsheets.

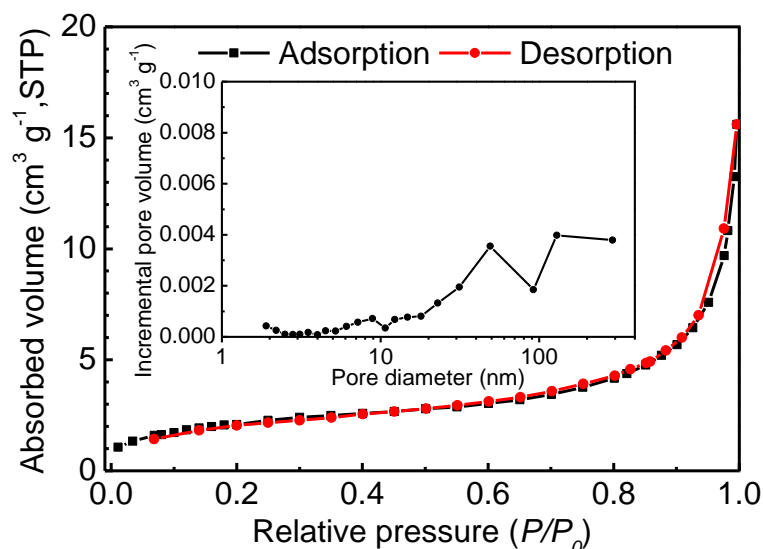


Figure S4. Nitrogen adsorption-desorption isotherms and pores size distribution (PSD, inset) of PPy microsheets.

As shown in **Fig. S3**, PPy microsheets show a type-II adsorption-desorption isothermal, which is typical for non-porous or macroporous adsorbent.¹ The pores size distribution (PSD, the inset of **Fig. S3**, calculated via BJH method by using nitrogen adsorption data) of PPy reveals the existence of a small amount of micropores and macropores, which arise from the interstitial pore space in particle aggregates. Calculated by the Brunauer-Emmett-Teller (BET) model, the specific surface area of PPy microsheets is $7.37 \text{ m}^2 \text{ g}^{-1}$.

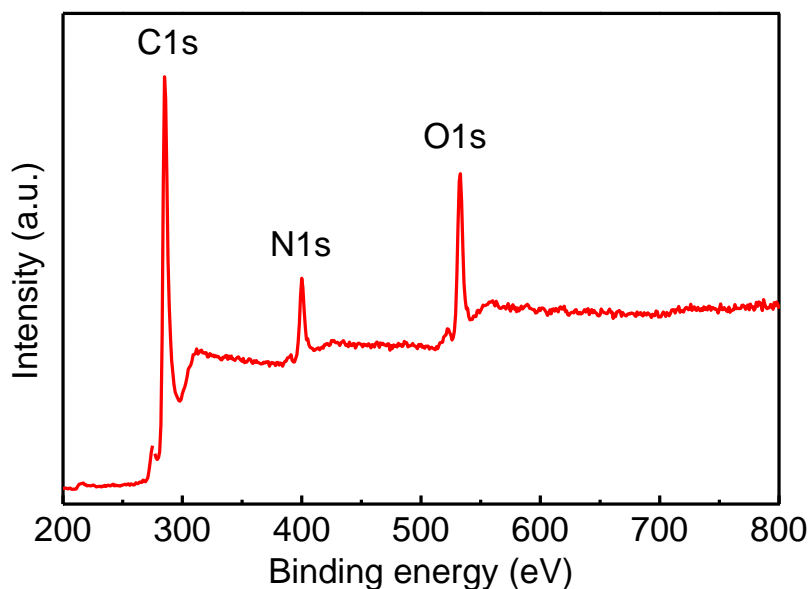


Figure S5. Survey XPS spectra of THPC.

As obtained using an element analyzer, THPC is composed of 77.0 wt.% C, 12.4 wt.% O, 7.7 wt.% N, 1.2 wt.% S and 1.5 wt.% H.

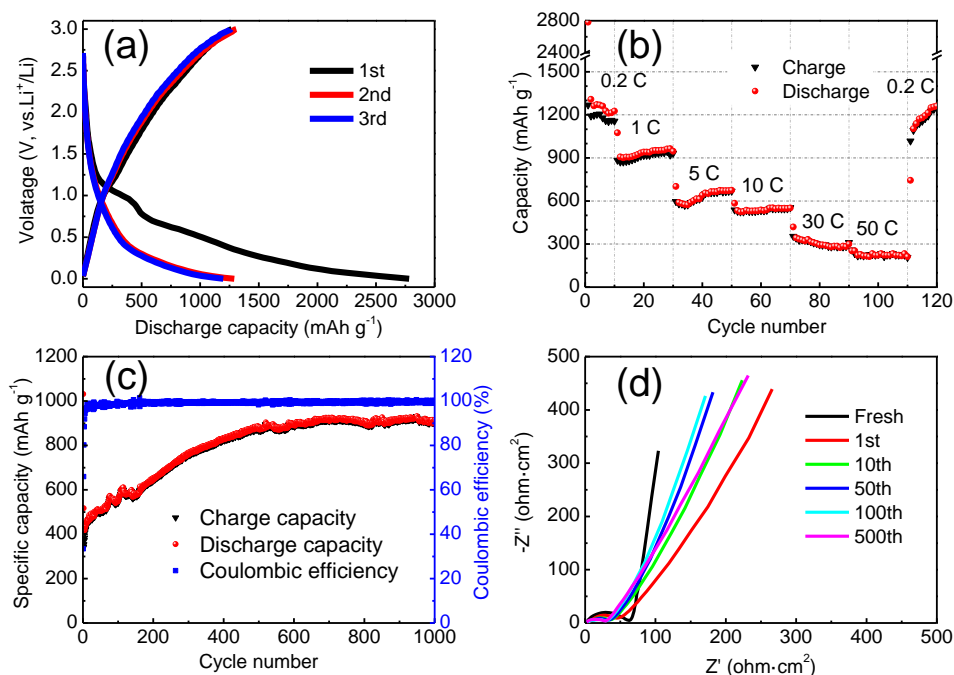


Figure S6 Electrochemical performances of THPC as anode electrode for lithium ion batteries: (a) discharge/charge curves at 0.2C; (b) capacity over cycling at different rates; (c) cyclability and coulombic efficiency at 5C; (d) impedance spectra of THPC after the 1st, 10th, 50th, 100th and 500th cycle at 5C.

THPC was also tested as anode electrode for lithium-ion batteries. Benefiting from its unique 3D hierarchical porous nanostructure and high-level N and O-doping, the THPC exhibits superior rate and cycling performances. As shown in **Figure S6b**, the reversible capacities are 1269, 944, 671, 553, 341 and 259 mAh g⁻¹ at 0.2, 1, 5, 10, 30 and 50 C (1 C = 372 mAh g⁻¹), respectively. When cycling at 5 C, the capacity is initially 344 mAh g⁻¹, gradually increases to 921 mAh g⁻¹ after 600 cycles and maintains up to 907 mAh g⁻¹ even after 1000 cycles (**Figure S6c**). The increasing capacity is due to the improvement of surface wetting between the electrode and electrolyte during extended cycling and the electroactivation process (**Figure S6d**). The obtained Li⁺-ion storage capability is extremely high among the carbonaceous anode materials.²⁻⁴

References

1. R. Pierotti and J. Rouquerol, *Pure Appl. Chem.*, 1985, **57**, 603-619.
2. J. Sun, H. Liu, X. Chen, D. G. Evans, W. Yang and X. Duan, *Adv. Mater.*, 2013, **25**, 1125-1130.
3. L. Qie, W. M. Chen, Z. H. Wang, Q. G. Shao, X. Li, L. X. Yuan, X. L. Hu, W. X. Zhang and Y. H. Huang, *Adv. Mater.*, 2012, **24**, 2047-2050.
4. W. C. Ren, Z. S. Wu, L. Xu, F. Li and H. M. Cheng, *Acs Nano*, 2011, **5**, 5463-5471.